

## KLOE RESULTS ON $\phi$ RADIATIVE DECAYS TO SCALAR AND PSEUDOSCALAR MESONS

CAMILLA DI DONATO FOR THE KLOE COLLABORATION<sup>1</sup>

*I.N.F.N. Sezione di Napoli, Italy*  
*E-mail address: camilla.didonato@na.infn.it*

Received 23 October 2007; Accepted 20 February 2008

Online 18 June 2008

We review recently published and preliminary results from the KLOE Collaboration on scalar and pseudoscalar mesons. We present the extraction of fundamental  $f_0(980)$  and  $a_0(980)$  parameters from the  $M_{\pi\pi}$  and  $M_{\eta\pi}$  spectrum with the first U.L. evaluation on the  $\phi \rightarrow K^0 \bar{K}^0 \gamma$  branching ratio. Concerning the pseudoscalar sector we present the results on  $\eta - \eta'$  mixing and  $\eta'$  gluonic content, with the most precise measurement of the  $\eta$  mass and the investigation of the  $\eta \rightarrow \pi\pi\pi$  dynamics from the Dalitz plot analysis. The study of the cross section for the processes  $e^+e^- \rightarrow \pi^+\pi^-\pi^0\pi^0/\pi^0\pi^0\gamma$  allow us to measure the OZI G-parity violating strongly suppressed decay  $\phi \rightarrow \omega\pi^0$ .

PACS numbers: 13.20.-v, 13.20.Jf, 14.40.-n

UDC 539.126

Keywords: radiative decays of  $\phi$  mesons, decays of other mesons, mesons

### 1. Introduction

The KLOE experiment has taken data at the  $\phi$ -factory DA $\phi$ NE [1], the Frascati  $e^+e^-$  collider, which operates at the center of mass energy  $\sqrt{s} = M_\phi \sim 1020$  MeV/ $c^2$ . The KLOE detector consists of a large cylindrical drift chamber (DC), surrounded by a fine sampling lead-scintillating-fiber electromagnetic calorimeter

<sup>1</sup>On behalf of the KLOE Collaboration: F. Ambrosino, A. Antonelli, M. Antonelli, C. Bacci, P. Beltrame, G. Bencivenni, S. Bertolucci, C. Bini, C. Bloise, S. Bocchetta, V. Bocci, F. Bossi, D. Bowring, P. Branchini, R. Caloi, P. Campana, G. Capon, T. Capussela, F. Ceradini, S. Chi, G. Chiefari, P. Ciambone, S. Conetti, E. De Lucia, A. De Santis, P. De Simone, G. De Zorzi, S. Dell'Agnello, A. Denig, A. Di Domenico, C. Di Donato, S. Di Falco, B. Di Micco, A. Doria, M. Dreucci, G. Felici, A. Ferrari, M. L. Ferrer, G. Finocchiaro, S. Fiore, C. Forti, P. Franzini, C. Gatti, P. Gauzzi, S. Giovannella, E. Gorini, E. Graziani, M. Incagli, W. Kluge, V. Kulikov, F. Lacava, G. Lanfranchi, J. Lee-Franzini, D. Leone, M. Martini, P. Massarotti, W. Mei, S. Meola, S. Miscetti, M. Moulson, S. Müller, F. Murtas, M. Napolitano, F. Nguyen, M. Palutan, E. Pasqualucci, A. Passeri, V. Patera, F. Perfetto, L. Pontecorvo, M. Primavera, P. Santangelo, E. Santovetti, G. Saracino, B. Sciascia, A. Sciubba, F. Scuri, I. Sfligoi, T. Spadaro, M. Testa, L. Tortora, P. Valente, B. Valeriani, G. Venanzoni, S. Veneziano, A. Ventura, R. Versaci and G. Xu.

(EMC) inserted in a 0.52 T magnetic field. The DC [2], 4 m diameter and 3.3 m long, has full stereo geometry and operates with a gas mixture of 90% helium and 10% isobutane. Momentum resolution is  $\sigma_{p_T}/p_T \leq 0.5\%$ . Position resolution in  $r - \phi$  is 150  $\mu\text{m}$  and  $\sigma_z \sim 2$  mm. Charged-track vertices are reconstructed with an accuracy of  $\sim 3$  mm. The EMC [3] is divided into a barrel and two endcaps and covers 98% of the solid angle. Arrival times of particles and space positions of the energy deposits are obtained from the signals collected at the two ends of the calorimeter modules; cells close in time and space are grouped into a calorimeter cluster. The cluster energy  $E$  is the sum of the cell energies, while the cluster time  $T$  and its position  $R$  are energy weighted averages. The respective resolutions are  $\sigma_E/E = 5.7\%/\sqrt{E(\text{GeV})}$  and  $\sigma_T = 57 \text{ ps}/\sqrt{E(\text{GeV})} \oplus 100 \text{ ps}$ . A photon is defined as a cluster energy release in EMC with time compatible with the speed of light and not associated to a charged track in the DC.

## 2. Scalar mesons at the $\phi$ -factory

The lighter mesons  $f_0(980)$  and  $a_0(980)$  are accessible through the  $\phi(1020) \rightarrow S\gamma$  radiative decays. KLOE has already published studies on  $\phi$  to  $f_0(980)\gamma$  and  $a_0(980)\gamma$  decays, with fully neutral final state, based on an integrated luminosity of 16  $\text{pb}^{-1}$  collected in 2000. Here we present the published results on  $\phi$  to  $f_0(980)\gamma$  decays with  $f_0(980)$  to  $\pi^+\pi^-$  [4], and to  $\pi^0\pi^0$  [5], based on data collected in 2001–2002, and preliminary results on  $\phi$  decays into  $a_0(980)\gamma$  with  $a_0(980) \rightarrow \eta\pi^0$  [6]. The  $\pi\pi$  and  $\eta\pi$  invariant masses spectra have been fitted to estimate the contribution from the scalar meson, using two different approaches in the description of the scalar amplitude:

- Kaon-loop model (KL) [7]: the  $\phi$  meson couples to  $S$  through a loop of  $K^+K^-$ ; the quantities  $g_{S\pi\pi}$ ,  $g_{SKK}$ ,  $M_S$  are free parameters in the fit;
- No-Structure model (NS) [8]: a direct coupling of the  $\phi$  to the  $S$  is assumed, with a subsequent coupling of the  $S$  to the  $\pi\pi$  pair. The  $S$  amplitude is a Breit-Wigner with a mass-dependent width.

We look for  $f_0(980) \rightarrow \pi^+\pi^-$  decays in events  $e^+e^- \rightarrow \pi^+\pi^-\gamma$ . The main contribution to the decay under study comes from  $e^+e^- \rightarrow \pi^+\pi^-\gamma$  events with a photon from initial state radiation (ISR), dominating for small photon polar angle  $\theta_\gamma$  or final state radiation (FSR). In the low-mass region, there is a small contribution from  $\phi \rightarrow \rho^\pm\pi^\pm$  with  $\rho^\pm \rightarrow \pi^\pm\gamma$ ; possible contribution from  $\phi \rightarrow \sigma(600)\gamma$  is considered. A sizeable interference term between FSR and  $f_0$  decay is expected because of the same quantum numbers of the  $\pi^+\pi^-$  pair ( $J^{PC} = 0^{++}$  for FSR and  $f_0$ ,  $J^{PC} = 1^{--}$  for ISR). The peak around 980 MeV (Fig. 1) is well interpreted as due to the  $\phi \rightarrow f_0(980)\gamma$  contribution, with a destructive interference with FSR; the non-scalar part is well described by the parametrization used, while we are not sensitive to the  $\rho\pi$  term. The KL fit is not sensitive to the  $\sigma$  contribution. The results of the fits suggest the  $f_0$  is strongly coupled to kaons. In Table 1 we show

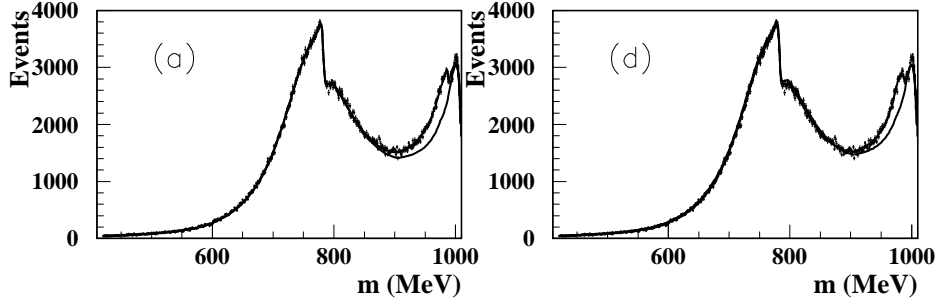


Fig. 1. Result of the fits: data spectrum compared with the fitting function and with the estimated non-scalar part of the function. Left: KL model; Right: NS model.

TABLE 1. Results of the KL-NS fit for  $f_0$ ; first two columns:  $f_0 \rightarrow \pi^+\pi^-$ , interval of maximal variations for the  $f_0$  parameters resulting from the systematic uncertainty studies done on both fits; second two columns:  $f_0 \rightarrow \pi^0\pi^0$ , the range comes from the combination of statistical and systematical errors.

Parameter	KL( $\pi^+\pi^-$ )	NS( $\pi^+\pi^-$ )	KL( $\pi^0\pi^0$ )	NS( $\pi^0\pi^0$ )
$m_{f_0}$ (MeV)	980-987	973-981	976-987	981-987
$g_{f_0 K^+ K^-}$ (GeV)	5.0-6.3	1.6-2.3	3.5-5.0	0.1-1.0
$g_{f_0 \pi^+ \pi^-}$ (GeV)	3.0-4.2	0.9-1.1	1.4-2.0	1.3-1.4
$R = g_{f_0 K^+ K^-}^2 / g_{f_0 \pi^+ \pi^-}^2$	2.2-2.8	2.6-4.4	3.0-7.3	0.1-1.0
$g_{\phi f_0 \gamma}$ (GeV $^{-1}$ )	–	1.2-2.0	–	2.5-2.7

intervals of maximal variations for the  $f_0$  parameters resulting from the systematic uncertainties of both fits, and Fig. 1 shows the fit to the spectra. We analyzed also the  $(\pi^+\pi^-)$  forward-backward asymmetry: a clear discrepancy is observed between data and simulation based only on the ISR and FSR amplitudes, while a prediction obtained including a scalar amplitude according to our results of KL fit describes qualitatively well both the effect in the  $f_0$  region and in the low-mass region.

Concerning the  $f_0(980) \rightarrow \pi^0\pi^0$  decay, the process under study is  $e^+e^- \rightarrow \pi^0\pi^0\gamma$ , and the two main contributions are: 1)  $e^+e^- \rightarrow \omega\pi^0 \rightarrow \pi^0\pi^0\gamma$  ( $\omega\pi$ ); 2)  $\phi \rightarrow S\gamma \rightarrow \pi^0\pi^0\gamma$  ( $S\gamma$ ); where  $S$  is  $\sigma$  or  $f_0(980)$ . In order to study the interference between the  $\omega\pi$  and  $S\gamma$  channels, we fit the whole Dalitz plot,  $m_{\pi^0\pi^0}$  versus  $m_{\pi^0\gamma}$ . The results from the fit with the two models are summarized in Table 1. The presence of  $\sigma(600)$  in KL model is needed to accurately describe the data, otherwise the probability of  $\chi^2$  becomes very poor; the fit with the NS approach is less stable. The results indicate a strong coupling of the  $f_0(980)$  to kaons, in agreement with our own analysis of the  $\pi^+\pi^-\gamma$  final state. By integrating the scalar amplitude over the  $\pi^0\pi^0$  invariant mass, we obtain an effective branching ratio  $BR(f_0 \rightarrow S\gamma \rightarrow$

$\pi^0\pi^0$ ) =  $(1.07 \pm 0.07) \times 10^{-4}$ , in agreement with the value expected from isospin by dividing by 2 the value obtained from the charged final state.

We look for  $a_0(980)$  in events from the process  $\phi \rightarrow \eta\pi^0\gamma$ . Events with  $\eta \rightarrow \gamma\gamma$  are characterized by five prompt photons in the final state, without any charged track in the drift chamber, and the main background processes are: 1)  $\phi \rightarrow \pi^0\pi^0\gamma$ , dominated by  $\phi \rightarrow f_0\gamma$ , 2)  $e^+e^- \rightarrow \omega\pi^0$  with  $\omega \rightarrow \pi^0\gamma$ , 3)  $\phi \rightarrow \eta\gamma$  with  $\eta \rightarrow \pi^0\pi^0\pi^0$ , and 4)  $\phi \rightarrow \eta\gamma$  with  $\eta \rightarrow \gamma\gamma$  (background from 3) and 4) is due to the photon merging or splitting). The background reduction proceeds through steps: (i) a kinematic fit on the events is performed, with the constraints of the 4-momentum conservation and  $|t-r/c|=0$  for each prompt photon; (ii) the best photon pairing to  $\pi^0$ 's and  $\eta$ 's and then (iii) a second kinematic fit is applied by imposing also the constraints of the masses of the intermediate particles. The  $\chi^2$  of these fits and other kinematical variables are used to reject the background events. The overall selection efficiency is 39%.

Events from decay  $\phi \rightarrow \eta\pi^0\gamma$  with  $\eta \rightarrow \pi^+\pi^-\pi^0$  are characterized by two tracks coming from the interaction region and five prompt photons. They are selected by requiring five prompt photons, according to the definition given above, and also two tracks in the drift chamber coming from a vertex close to the beam interaction point. There are no other relevant processes with exactly the same final state, the background comes mainly from:  $e^+e^- \rightarrow \omega\pi^0$  with  $\omega \rightarrow \pi^+\pi^-\pi^0$  and  $\phi \rightarrow K_S K_L$ . The background reduction is based on kinematic fit using 4-momentum conservation and  $\pi^0$ ,  $\eta$  invariant masses. The overall efficiency for the signal is close to 20%, while the residual background is  $\approx 15\%$ . The number of selected events is 29601 for the fully neutral final state, the total background amounts to  $16332 \pm 86$  events, while in the charged final state, 4180 were selected with  $542 \pm 57$  background events. To obtain the branching ratio, the number of events has been normalized to the number of  $\phi \rightarrow \eta\gamma$  with  $\eta \rightarrow \pi^0\pi^0\pi^0$  events selected in the same analyzed sample. We obtain the two values in good agreement:

$$\begin{aligned} BR(\phi \rightarrow \eta\pi^0\gamma) &= (6.92 \pm 0.17) \times 10^{-5} & (\eta \rightarrow \gamma\gamma) \\ BR(\phi \rightarrow \eta\pi^0\gamma) &= (7.19 \pm 0.24) \times 10^{-5} & (\eta \rightarrow \pi^+\pi^-\pi^0) \end{aligned}$$

A combined fit of the two spectra with the same parameters has been performed; the parameters values are reported in Table 2.

The fits yield also the value of  $BR(\eta \rightarrow \gamma\gamma)/BR(\eta \rightarrow \pi^+\pi^-\pi^0) = 1.69 \pm 0.04$  which agrees well with the expected value ( $1.73 \pm 0.03$  from PDG [9]).

Close to these issues, KLOE has searched for the  $\phi \rightarrow K^0\bar{K}^0\gamma$  decay [10] using a sample of  $1.4 \text{ fb}^{-1}$ , the value of the branching ratio gives relevant information on the scalar structure because it is expected to proceed mainly through  $\phi \rightarrow (f_0 + a_0)\gamma$ . It has never been searched before, while many theory models predict a  $BR \sim 10^{-8}$ . Due to its clean topology, we selected the channel  $K_S K_S \rightarrow \pi^+\pi^-\pi^+\pi^-$ . The main background comes from  $K_S K_L + \text{ISR/FSR}$ . We observed one event on data, with no events in Monte Carlo background and then we set a preliminary value of the U.L.  $BR(\phi \rightarrow K^0\bar{K}^0\gamma) < 1.8 \cdot 10^{-8}$ , 90% C.L.

TABLE 2. The KL-NS fit results for  $a_0$ : systematics of the parameters are not included.

Parameter	KL	NS
$M_{a_0}$ (MeV)	$983 \pm 1$	983 (fixed)
$g_{a_0 K^+ K^-}$ (GeV)	$2.16 \pm 0.04$	$1.57 \pm 0.13$
$g_{a_0 \eta \pi^0}$ (GeV)	$2.8 \pm 0.1$	$2.2 \pm 0.1$
$g_{\phi a_0 \gamma}$ (GeV $^{-1}$ )	—	$1.61 \pm 0.05$
$\delta(^{\circ})$	$222 \pm 12$	—
$Br(\phi \rightarrow \rho \pi^0 \rightarrow \eta \pi^0 \gamma) \times 10^6$	$0.9 \pm 0.4$	4.1 (fixed)
$Br(\eta \rightarrow \gamma \gamma) / Br(\eta \rightarrow \pi^+ \pi^- \pi^0)$	$1.69 \pm 0.04$	$1.69 \pm 0.04$
$\chi^2 / Ndf$	156.6/136	146.8/134
$P(\chi^2, ndf)$	11%	21%

### 3. Pseudoscalar mesons

In the pseudoscalar sector, we have investigated the  $\eta - \eta'$  mixing, the  $\eta$  mass and the  $\eta \rightarrow \pi\pi\pi$  dynamics with the Dalitz plot technique. The ratio  $R_\phi = BR(\phi \rightarrow \eta' \gamma) / BR(\phi \rightarrow \eta \gamma)$  can be related to the  $\eta - \eta'$  mixing angle in the flavor basis [12–17]. Moreover, combined with other constraints  $R_\phi$  can be related also to the gluonium content of the  $\eta'$  meson [14, 18]. Analyzing 427 pb $^{-1}$  (2001–2002), we have looked for  $\eta' \gamma$  in the  $\pi^+ \pi^- 7\gamma$ 's final state [19], with two different secondary decay chains: 1)  $\eta' \rightarrow \pi^+ \pi^- \eta$  and  $\eta \rightarrow \pi^0 \pi^0 \pi^0$  (CH); 2)  $\eta' \rightarrow \pi^0 \pi^0 \eta$  and  $\eta \rightarrow \pi^+ \pi^- \pi^0$  (NEU).  $\phi \rightarrow \eta \gamma$  events used for normalization have been searched in the  $7\gamma$ 's final state, with  $\eta \rightarrow \pi^0 \pi^0 \pi^0$ , which is practically background free. Processes with  $\phi \rightarrow K_S K_L$ , where the  $K_L$  decays near the beam interaction point, can mimic the final state with  $\pi^+ \pi^- 7\gamma$ 's because of the presence of an additional photon due either to machine background or splitting clusters. We select 3750  $\eta'$  candidate events and the expected background is  $N_b = 345$ . The total number of events from processes (CH) and (NEU), after background subtraction, is  $N_{\eta' \gamma} = 3405$ . For the process  $\phi \rightarrow \eta \gamma$  we select  $N_{\eta \gamma} = 1665000$  events. The ratio of the two branching fractions and the branching ratio of  $\phi \rightarrow \eta' \gamma$  have been evaluated:

$$R_\phi = (4.77 \pm 0.09_{\text{stat}} \pm 0.19_{\text{syst}}) \cdot 10^{-3} \Rightarrow BR(\phi \rightarrow \eta' \gamma) = (6.20 \pm 0.11_{\text{stat}} \pm 0.25_{\text{syst}}) \cdot 10^{-5}$$

the branching ratio comes from  $R_\phi$  times the  $BR(\phi \rightarrow \eta \gamma) = (1.301 \pm 0.024)\%$  (PDG'06 [9]). Using the approach of Refs. [16, 17], we extract the pseudoscalar mixing angle from  $R_\phi$ :  $\phi_P = (41.4 \pm 0.3_{\text{stat}} \pm 0.7_{\text{sys}} \pm 0.6_{\text{th}})^{\circ}$ .

The  $\eta'$  meson is a good candidate to have a sizeable gluonium content, we can have  $|\eta'\rangle = X_{\eta'} |q\bar{q}\rangle + Y_{\eta'} |s\bar{s}\rangle + Z_{\eta'} |gluon\rangle$ , where the  $Z_{\eta'}$  parameter takes in to account a possible mixing with gluonium. The normalization implies  $X_{\eta'}^2 + Y_{\eta'}^2 + Z_{\eta'}^2 = 1$  with  $X_{\eta'} = \cos \phi_G \sin \phi_P$ ,  $Y_{\eta'} = \cos \phi_G \cos \phi_P$  and  $Z_{\eta'} = \sin \phi_G$ , where

$\phi_G$  is the mixing angle for the gluonium contribution. Possible gluonium content of the  $\eta'$  meson corresponds to non-zero value for  $Z_{\eta'}^2$ . Introducing other constraints on  $X_{\eta'}$  and  $Y_{\eta'}$  [14, 17, 18], as:  $\Gamma(\eta' \rightarrow \gamma\gamma)/\Gamma(\pi^0 \rightarrow \gamma\gamma)$ ;  $\Gamma(\eta' \rightarrow \rho\gamma)/\Gamma(\omega \rightarrow \pi^0\gamma)$ ;  $\Gamma(\eta' \rightarrow \omega\gamma)/\Gamma(\omega \rightarrow \pi^0\gamma)$ , and allowing for gluonium, we minimized the  $\chi^2$ , function of  $(\phi_P, \phi_G)$ , to determine  $Z_{\eta'}^2$  and  $\phi_P$ . The solution in the hypothesis of no gluonium content, i.e.  $Z_{\eta'}^2 = 0$ , yields  $\phi_P = (41.5_{-0.7}^{+0.6})^\circ$ ; the  $\chi^2$  quality is bad, while allowing for gluonium the  $\chi^2$  quality is good,  $P(\chi^2/d.f.) = 0.49$  and the results are  $\phi_P = (39.7 \pm 0.7)^\circ$  with  $Z_{\eta'}^2 = 0.14 \pm 0.04$ . Our analysis indicates a  $3\sigma$  evidence for the  $\eta'$  gluonium content.

Concerning the  $\eta$  meson, a large discrepancy ( $8\sigma$ ) between the two most precise  $\eta$  mass measurement, from the GEM collaboration [20] and the NA48 [21], has suggested KLOE to perform a new measurement [22]. The process studied is  $\phi \rightarrow \eta\gamma$ ,  $\eta \rightarrow \gamma\gamma$  and also  $\phi \rightarrow \pi^0\gamma$  to obtain the ratio of the two masses  $r = m_\eta/m_{\pi^0}$ . The  $\eta$  mass is obtained from the  $\gamma\gamma$  invariant mass distribution. To improve the photon energy measurement, a kinematic fit is performed with constraints from energy-momentum conservation. The data sample (2001–2002) has been divided into eight sub-periods, in order to determine the value of  $m_{\pi^0}$ ,  $m_\eta$  and  $r$  as a function of sub-period. The obtained values have been fitted with a constant. To extract the  $\eta$  mass value we can use our measured ratio  $r = 4.0610 \pm 0.0004_{\text{stat}} \pm 0.0014_{\text{syst}}$  and the PDG'06 value of the  $\pi^0$  mass; we obtain  $m_\eta = (548.140 \pm 0.050_{\text{stat}} \pm 0.190_{\text{syst}})$  MeV.

An alternative procedure is to calibrate our  $\sqrt{s}$  with high precision. We compare the  $m_\phi$  value measured by CMD-2 [23] to the one obtained fitting the  $\phi$  resonance curve from KLOE, with the CMD-2 parametrization. The difference between the two value ( $m_{\phi, \text{CMD-2}} = (1019.483 \pm 0.011_{\text{stat}} \pm 0.025_{\text{syst}})$  MeV,  $m_{\phi, \text{KLOE}} = (1019.329 \pm 0.011)$  MeV) sets our absolute  $\sqrt{s}$  calibration. The KLOE measurement confirms the NA48 measurement within 0.24 standard deviations and disagrees with GEM one by seven standard deviations:

$$m_\eta = (547.873 \pm 0.007_{\text{stat}} \pm 0.031_{\text{syst}}) \text{ MeV and}$$

$$m_{\pi^0} = (134.906 \pm 0.012_{\text{stat}} \pm 0.048_{\text{syst}}) \text{ MeV}$$

The huge amount of data collected by KLOE allowed us to investigate the  $\eta \rightarrow \pi\pi\pi$  dynamics with the Dalitz plot technique. The decay of isoscalar  $\eta$  into three pions occurs, besides a negligible electromagnetic contribution of the second order [24], through isospin violation, and as a consequence the decay amplitude is proportional to the  $d - u$  quark mass difference; from the decay rate  $\Gamma(\eta \rightarrow \pi\pi\pi)$  the quark mass ratio can be calculated.

The  $\eta$  meson is produced in the process  $\phi \rightarrow \eta\gamma$ , where the recoil photon ( $E_\gamma = 363$  MeV) is monochromatic and easily selected, the background is at the level of few per mill for both channels studied:  $\eta \rightarrow \pi^+\pi^-\pi^0$  and  $\eta \rightarrow \pi^0\pi^0\pi^0$ . The Dalitz plot of  $\eta \rightarrow \pi^+\pi^-\pi^0$  is described by two kinematic variables,  $X = \sqrt{3}(T_+ - T_-)/Q_\eta$  and  $Y = 3T_0/Q_\eta - 1$ , with  $Q_\eta = m_\eta - 2m_{\pi^+} - m_{\pi^0}$ . The efficiency, as function of the

Dalitz plot variables, is almost flat all over the kinematically allowed region, and the mean value is 33%. The measured distribution is expanded around  $X = Y = 0$ , the center of the Dalitz plot, in powers of  $X$  and  $Y$ , and the parameters of the expansion are fitted to the experimental data:  $|A(X, Y)|^2 \simeq 1 + aY + bY^2 + cX + dX^2 + eXY + fY^3$ . Any odd power of  $X$  contributing to  $|A(X, Y)|^2$  would imply violation of charge conjugation. The fit results are reported in Table 3: they show no C-violation; the quadratic slope in  $X$  is different from zero and for the first time the sensitivity to a cubic term of the expansion has been reached.

TABLE 3. Results for the slope parameter of Dalitz Plot; the first line reports the parameters values with statistical error, while the second indicates the systematic one. Systematic errors take into account efficiency evaluation, resolution effects and background contamination.

a	b	c	d	e	f
$-1.090 \pm 0.005$	$0.124 \pm 0.006$	$0.002 \pm 0.003$	$0.057 \pm 0.006$	$-0.006 \pm 0.007$	$0.14 \pm 0.01$
$+0.008$ $-0.019$	$\pm 0.010$	$\pm 0.001$	$+0.007$ $-0.016$	$+0.005$ $-0.003$	$\pm 0.02$

Possible contributions to C violation in amplitudes with fixed  $\Delta I$  have been investigated: the left-right asymmetry  $A_{LR} = (0.09 \pm 0.10^{+0.09}_{-0.14}) \times 10^{-2}$ , the quadrants  $A_Q = (-0.05 \pm 0.10^{+0.03}_{-0.05}) \times 10^{-2}$  and the sextant  $A_S = (0.08 \pm 0.10^{+0.08}_{-0.13}) \times 10^{-2}$ , are in agreement with the null value of the  $c$  and  $e$  parameters in the fit.

The Dalitz plot of  $\eta \rightarrow \pi^0 \pi^0 \pi^0$  is described by a single quadratic slope parameter  $\alpha$ :  $|A(z)|^2 \simeq 1 + 2\alpha z$ , where  $z = \rho^2 / \rho_{\max}^2$  is the square ratio of the distance of a point from the Dalitz plot center,  $\rho$ , to the maximum kinematically allowed distance,  $\rho_{\max}^2$ . A first kinematic fit has been performed to improve photon energy resolution, followed by a photons to  $\pi^0$  pairing procedure and a second fit, constraining also the  $\pi^0$  mass. In order to estimate  $\alpha$ , an unbinned likelihood function is built by convoluting the event density with the resolution function and correcting for the probability of wrong photon pairing in  $\pi^0$ 's. Using a sample with high purity on pairing and fitting in the range  $0 \leq z \leq 1$ , we found a preliminary result [25] only marginally compatible with the Crystal Ball one [26]. Further systematic checks have shown a relevant dependence of  $\alpha$  on the fitting range. Moreover, the low purity / high statistics sample shows two different slopes (see Fig. 2, left) in the Data-MC ratio of the  $z$  distribution. With a dedicated simulation, we have realized that this is essentially due to a different value of invariant mass of three pion system ( $\pi^0 \pi^0 \pi^0$ ) in the Monte Carlo generator, with respect to the one recently measured [22] by our experiment. As a consequence, the accessible phase space on data is larger than the one on Monte Carlo simulation. This was not evident in the high purity / low statistics sample used for the preliminary result quoted. A new evaluation of  $\alpha$  has been obtained after a kinematic fit with an additional constraint on the  $\eta$  mass, which recover this effect. In this way, good stability with respect to the

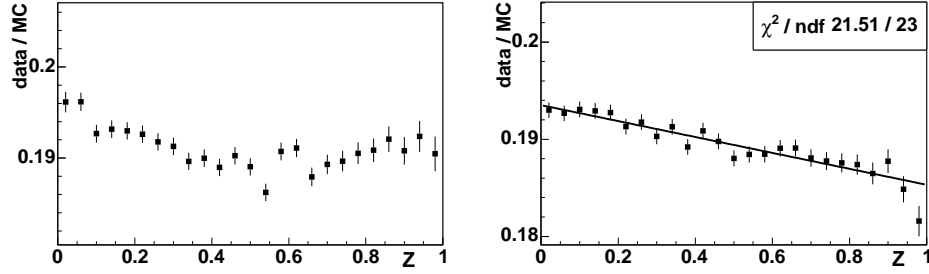


Fig. 2. Left: Data-Monte Carlo ratio of the  $z$  distribution. The MC distribution is pure phase space; right: Data-Monte Carlo ratio of the  $z$  distribution after the kinematic fit with  $\eta$  mass constraint; Monte Carlo with  $\eta$  mass value measured by KLOE.

fit range is observed, and the linearity of the Data-MC ratio of the  $z$  distribution has been recovered, (see Fig. 2, right). We give the final result fitting in the region  $z \in [0, 0.7]$ . We quote as new preliminary result for the slope parameter  $\alpha$ , the one obtained with the Medium Purity sample, (about  $65 \times 10^4$   $\eta \rightarrow 3\pi^0$  decays); the result, including the statistical uncertainty from the fit and the evaluated systematic error is:

$$\alpha = -0.027 \pm 0.004 \text{ (stat)} \begin{matrix} +0.004 \\ -0.006 \end{matrix} \text{ (syst)}, \quad (1)$$

compatible within errors with the result from Crystal Ball [26], based on  $10^6$  events,  $\alpha = -0.031 \pm 0.004$ , and the calculations from the chiral unitary approach [27].

#### 4. $e^+e^- \rightarrow \omega\pi^0$

Using  $600 \text{ pb}^{-1}$ , we have studied the production cross section of  $\pi^+\pi^-\pi^0\pi^0$  and  $\pi^0\pi^0\gamma$  final states in  $e^+e^-$  collisions at the center-of-mass energies between 1000 and 1030 MeV. In this energy range, the  $e^+e^- \rightarrow \pi^+\pi^-\pi^0\pi^0$  production cross section is largely dominated by the non-resonant processes  $e^+e^- \rightarrow \rho/\rho' \rightarrow \omega\pi^0$ , with a contribution from the OZI and G-parity violating decay  $\phi \rightarrow \omega\pi^0$ , which is strongly suppressed. The latter process can be observed through the interference pattern with the former one, which shows up as a dip in the production cross section as a function of  $\sqrt{s}$ . The scenario for  $e^+e^- \rightarrow \pi^0\pi^0\gamma$  is much more complicated due to the contributions from  $\phi \rightarrow \rho\pi$  and  $\phi \rightarrow S\gamma$  intermediate states. Contribution from  $\phi \rightarrow S\gamma$  process will be neglected, because the interference with  $e^+e^- \rightarrow \omega\pi^0$  events, evaluated by fitting the  $M_{\pi\pi} - M_{\pi\gamma}$  Dalitz plot is small [5]. The dependence of the cross section on the center-of-mass energy can be parameterized as:

$$\sigma(\sqrt{s}) = \sigma_0(\sqrt{s}) \cdot \left| 1 - Z \frac{M_\phi \Gamma_\phi}{D_\phi} \right|, \quad \sigma_0(\sqrt{s}) = \sigma_0 + \sigma'(\sqrt{s} - M_\phi). \quad (2)$$

For the non-resonant cross section  $\sigma_0(\sqrt{s})$  we have used the linear approximation;  $Z$  is the complex interference pattern and  $M_\phi, \Gamma_\phi$  and  $D_\phi$  are the mass, the width



and the propagator of the  $\phi$ , respectively. The measured values of visible cross section are fitted with the parametrization (2), convoluted with a radiator function [28]. The preliminary results for the two fits are shown in Table 4 and in Fig. 3 and Fig. 4.

TABLE 4. Fit results for the  $e^+e^- \rightarrow \pi^+\pi^-\pi^0\pi^0$  cross section (left) and for the  $e^+e^- \rightarrow \pi^0\pi^0\gamma$  cross section (right).

Parameter	$(e^+e^- \rightarrow \pi^+\pi^-\pi^0\pi^0)$	Parameter	$(e^+e^- \rightarrow \pi^0\pi^0\gamma)$
$\sigma_0^{4\pi}$ (nb)	$8.12 \pm 0.14$	$\sigma_0^{\pi\pi\gamma}$ (nb)	$0.776 \pm 0.012$
$\Re(Z_{4\pi})$	$0.097 \pm 0.012$	$\Re(Z_{\pi\pi\gamma})$	$0.013 \pm 0.013$
$\Im(Z_{4\pi})$	$-0.133 \pm 0.009$	$\Im(Z_{\pi\pi\gamma})$	$-0.155 \pm 0.007$
$\sigma'_{4\pi}$ (nb/MeV)	$0.072 \pm 0.008$	$\sigma'_{\pi\pi\gamma}$ (nb/MeV)	$0.0079 \pm 0.0006$

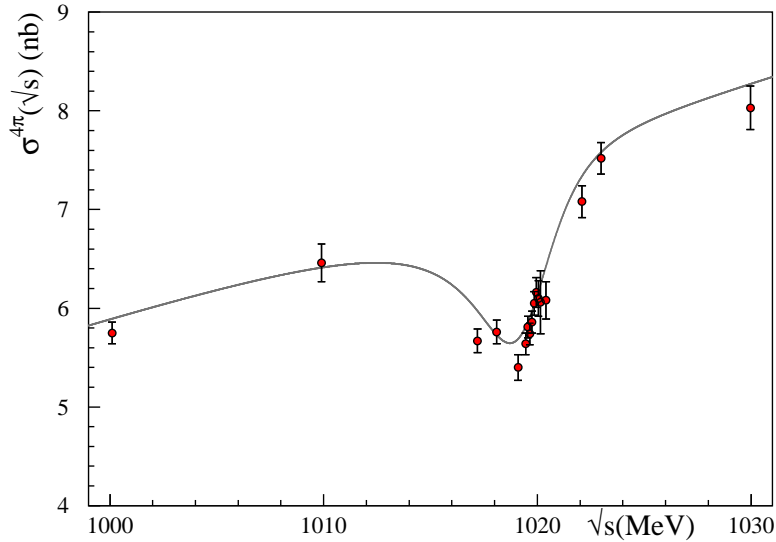


Fig. 3. Cross section fit results for the  $e^+e^- \rightarrow \pi^+\pi^-\pi^0\pi^0$ ; dots are data, solid lines resulting fit function.

From the ratio of the two  $\sigma_0$ , taking into account the phase space difference between the two decays, we extract the ratio of the partial widths:  $\Gamma(\omega \rightarrow \pi^0\gamma)/\Gamma(\omega \rightarrow \pi^+\pi^-\pi^0) = 0.0934 \pm 0.0021$ . The  $\pi^0\gamma$  and the  $\pi^+\pi^-\pi^0$  represent 98% of the  $\omega$  decay channels; therefore from the previous result and the remaining rare  $\omega$  decays, by constraining the sum of branching ratios to one, we obtain:  $BR(\omega \rightarrow \pi^0\gamma) = (8.40 \pm 0.19)\%$  and  $BR(\omega \rightarrow \pi^+\pi^-\pi^0) = (89.94 \pm 0.23)\%$ , with a correlation of 82%. We extract also the branching ratio for  $\phi \rightarrow \omega\pi^0$  using

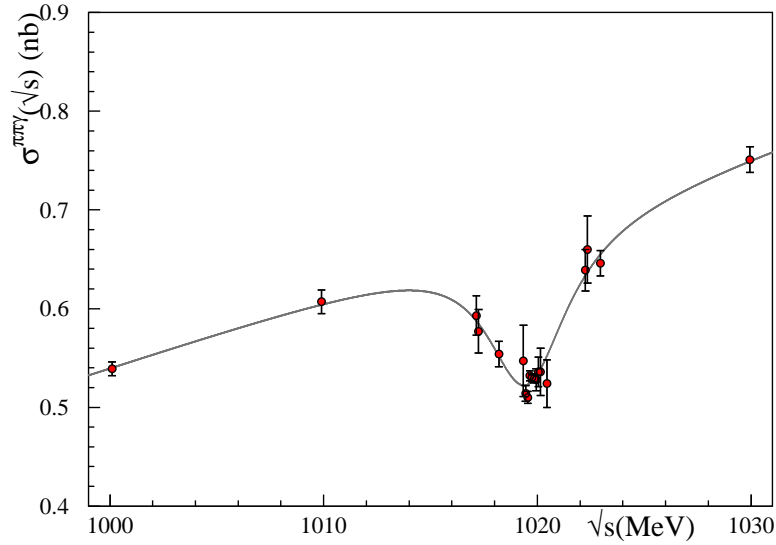


Fig. 4. Cross section fit results for the  $e^+e^- \rightarrow \pi^0\pi^0\gamma$ ; dots are data, solid lines resulting fit function.

the relation

$$BR(\phi \rightarrow \omega\pi^0) = \frac{\sigma_0(m_\phi) |Z_{4\pi}|^2}{\sigma_\phi}. \quad (3)$$

The resulting value  $BR(\phi \rightarrow \omega\pi^0) = (5.63 \pm 0.70) \times 10^{-5}$  is in agreement with the previous measurement from SND experiment [29].

## 5. Conclusions

The KLOE collaboration studied  $\phi \rightarrow S\gamma$  in different final states to extract the relevant couplings related to the two models, the KL and NS, advocated to describe the scalar amplitude. The experimental data are reasonably described by the models and the results, large  $BR(\phi \rightarrow S\gamma)$ , large coupling to  $\phi$  and large coupling to  $KK$ , at least for  $f_0$ , and suggest a non  $q\bar{q}$  structure of  $f_0(980)$  and  $a_0(980)$ . The data indicate the  $\sigma$  meson as a contribution needed in  $\pi^0\pi^0\gamma$  analysis, not in  $\pi^+\pi^-\gamma$ . A combined analysis of  $f_0 \rightarrow \pi^0\pi^0$  and  $f_0 \rightarrow \pi^+\pi^-$  is under way. Preliminary results are available also on  $a_0$  properties.

The KLOE data provided interesting results also on pseudoscalar mesons, as the pseudoscalar mixing angle measurement and the most precise  $\eta$  mass measurement. New precise measurement of Dalitz plot slope parameter of  $\eta \rightarrow \pi^+\pi^-\pi^0$  and  $\eta \rightarrow \pi^0\pi^0\pi^0$  are available with most stringent limit on C violation from  $\eta \rightarrow \pi^+\pi^-\pi^0$  asymmetries. Moreover, the result from the fit to the observed interference pattern around  $M_\phi$  for  $e^+e^- \rightarrow \pi^+\pi^-\pi^0\pi^0/\pi^0\pi^0\gamma$  allowed to extract the branching fraction for the OZI and G-parity violating  $\phi \rightarrow \omega\pi^0$  decay.

## References

- [1] S. Guiducci et al., Proc. 2001 Particle Accelerator Conf., Chicago, Illinois (USA)), eds. P. Lucas and S. Webber (2001) p. 353.
- [2] M. Adinolfi et al. [KLOE Collaboration], Nucl. Instrum. Meth. A **488** (2002) 51.
- [3] M. Adinolfi et al. [KLOE Collaboration] Nucl. Instrum. Meth. A **482** (2002) 364.
- [4] F. Ambrosino et al. [KLOE Collaboration], Phys. Lett. B **634** (2006) 148.
- [5] F. Ambrosino et al. [KLOE Collaboration], Eur. Phys. J. C **49** (2007) 473.
- [6] F. Ambrosino et al. [KLOE Collaboration], arXiv:0707.4609 [hep-ex].
- [7] N. N. Achasov and V. N. Ivanchenko, Nucl. Phys. B **315** (1989) 465.
- [8] G. Isidori, L. Maiani and S. Pacetti, private communication.
- [9] W.-M. Yao et al., J. Phys. G **33** (2006) 1.
- [10] F. Ambrosino et al. [KLOE Collaboration], arXiv:0707.4148 [hep-ex].
- [11] M. Benayoun et al., Phys. Rev. D **59** (1999) 114027.
- [12] T. Feldmann, Int. J. Mod. Phys. A **15** (2000) 159.
- [13] C. Becchi and G. Morpurgo, Phys. Rev. B **687** (1965) 140.
- [14] J. L. Rosner, Phys. Rev. D **27** (1983) 1101.
- [15] P. Ball, J. M. Frere and M. Tytgat, Phys. Lett. B **365** (1996) 367.
- [16] A. Bramon, R. Escribano and M. D. Scadron, Eur. Phys. J. C **7** (1999) 271.
- [17] A. Bramon, R. Escribano and M. D. Scadron, Phys. Lett. B **503** (2001) 271.
- [18] E. Kou, Phys. Rev. D **63** (2001) 54027.
- [19] F. Ambrosino et al. [KLOE Collaboration], Phys. Lett. B **648** (2007) 267.
- [20] M. Abdel-Bary et al., Phys. Lett. B **619** (2005) 281.
- [21] A. Lai et al., Phys. Lett. B **533** (2002) 196.
- [22] F. Ambrosino et al. [KLOE Collaboration], arXiv:0707.4616 [hep-ex].
- [23] R. R. Akhmetzin et al., Phys. Lett. B **578** (2004) 285.
- [24] R. Baur, J. Kambor and D. Wyler, Nucl. Phys. B **460** (1966) 127.
- [25] T. Capussela on Behalf of the KLOE Collaboration, Acta Phys. Slov. **56** (2005) 341.
- [26] Crystal Ball Collaboration, Phys. Rev. Lett. **87** (2001) 19.
- [27] B. Borasoy and R. Nissler, [hep-ph/0510384 v2].
- [28] M. Greco et al., Phys. Lett. B **318** (1993) 635.
- [29] V. M. Aulchenko et al., J. Exp. Th. Phys. **90** (2000) 927.

ISHODI MJERENJA KLOE ZA RADIJATIVNE RASPADE  $\phi$  U SKALARNE I PSEUDOSKALARNE MESONE

Dajemo pregled nedavno objavljenih i prethodnih ishoda mjerenja Suradnje KLOE za skalarne i pseudoskalarne mezone. Predstavljamo izvođenje osnovnih parametara  $f_0(980)$  i  $a_0(980)$  iz spektra  $M_{\pi\pi}$  i  $M_{\eta\pi}$  i dajemo prvu gornju granicu za omjer grananja  $\phi \rightarrow K^0 \bar{K}^0 \gamma$ . Što se tiče pseudoskalara, dajemo ishode za miješanje  $\eta - \eta'$  i za gluonski sadržaj u  $\eta'$ , s najtočnijim mjerenjem mase  $\eta$  i istraživanjem dinamike  $\eta \rightarrow \pi\pi\pi$  primjenom analize Dalitzovim dijagramom. Proučavanje udarnih presjeka procesa  $e^+e^- \rightarrow \pi^+\pi^-\pi^0\pi^0/\pi^0\pi^0\gamma$  omogućilo je određivanje raspada  $\phi \rightarrow \omega\pi^0$  koji je snažno potisnut jer narušava OZI i G-parnost.